Bulletin of Earth Sciences of Thailand

MAPPING OF FAULT SYSTEM RELATED TO SALT MOVEMENT IN VOLVE FIELD, OFFSHORE NORWAY, NORTH SEA

Teerapong Jiratitipat*

Department of Geology, Faculty of Science, Chulalongkorn University, Bangkok 10330, Thailand
*Corresponding author email: Teerapongji@outlook.com

Abstract

3D seismic data and well data of the Volve field are integrated with seismic attributes to determine the tectonic evolution and fault system which were caused by salt movement during Triaasic and Jurassic periods. In the methodology, there are many attributes for seismic enhancement, fault imaging, fault enhancment and fault-patch extraction. Median filter is used for seismic enhancement. Variance and Chaos attributes are used to imaging faults and the fault image in Varinace attribute presented better images than Chaos attribute, thus the result of Variance attribute volume is processed in the next step. Edge Evidence and Ant-Tracking attributes are used to enhance fault image. The results present clear fault features of the Volve field. Automatic Fault Extraction (AFE) feature in the softwere does not work in this field. It may be due to a large number of fault-patches and high range of fault values in the Ant-Tracking attribute. The result of this study presents the fault image clearly in the Volve field. Moreover, the fault orientation of Triassic section are in NW-SE and NE-SW directions. The NE-SW direction is along the same direction with the major fault trend of the South Viking Graben. Although, there are a minor shift from the fault orientation in the Upper Permian section. It may be caused by salt movement. At last, the fault images in the Ant-Tracking attribute present low tectonic activity during Jurassic period due to lack of faults in the Jurassic section.

Keywords: Seismic attributes, Volve field, Salt Identification

1. Introduction

Volve oil field was discovered in 1993 by Statoil company during drilling of 015/09-19SR well. It is in Block 15/9, offshore Norway, North Sea. Volve field came on-stream in February 2008 and abandoned in September 2016. Volve field is in the central part of the North Sea, about 10 km east of Sleipner West Field (Figure 1). It is a small dome shaped structure with dimension of 2 x 3 km. Evaporite deformation is an important event in reservoir distribution and trap structure of the Field. The main reservoir interval was Hugin formation. It is Jurassic shallow marine sandstone. The thickness of reservoir varies from 20 m at the top of the crest and increases up to 100 m on the flank of the structure. The reservoir structures featured by minibasins, dome structure and fault system were formed by Zechstein salt movement during Triassic and Jurassic. This study applies seismic attributes with 3D seismic data to explain the fault system that formed by Zechstein salt movement. The result will support the understanding of Triassic and Jurassic fault system evolution in the Volve field and can be applied to similar Fields in the North Sea

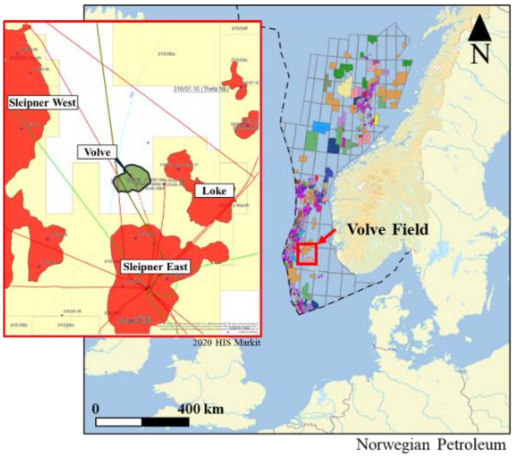

Figure 1. Location of study area, Volve field, North Sea, Norway.

2. General Geology

2.1 Geological Structure

Volve field is located near to junction of 3 major structures (Figure 2.1) in North Sea; South Viking Graben, Horda platform and Norwegian-Danish basin. Volve field is located in Utsira high which is limited by intersection of

NE-SW trending fault of the Viking graben and NW-SE trending fault parallel to the Norwegian-Danish basin axis. The NE-SE fault called "Caledonoid" fault controls the west boundary of the Viking graben. The NW-SE trending fault of Norwegian-Danish basin was formed by a pre-Permian fracture related to the zone of weakness forming the southwest boundary of the Fennoscanian-Russian platform which is called "Tornquist zone". In Volve field, NE-SW trending fault is the major fault system. It separates Sleipner Terrace from the Utsira high. Volve field is located in the South Viking graben on the eastern upthrown side of Gamma high fault which is the south extension of the Utsira high (Pegrum, 1984). The NE-SW main fault dips to the west with a large displacement in the western part of Volve field. The N-S minor faults with small displacement are in the eastern part.

Volve field had local tectonic event caused by Late Permian salt movement during Triassic and Jurassic periods that affected the geological structure and sedimentation. Examples of these structures are dome structure, minibasins, fault system, and changes in sedimentary facies. During the Triassic, a series of minibasins formed due to salt formation in Zechstein Supergroup movement. Afterwards, in the Jurassic period, a series of secondary minibasins developed as underlying salt walls collapsed. The minibasins are bound by salt cored structural highs. Salt body shape is sub-circular to elongate which causes complex subaerial topography development and a resulting submarine bathymetry on the SW margin of the Utsira High. The changes in salt shape can be related to partial dissolution of salt; differential erosion of the salt walls and adjacent Triassic-filled minibasins; or salt remigration caused by salt extension or sediment loading (Jackson, 2010).

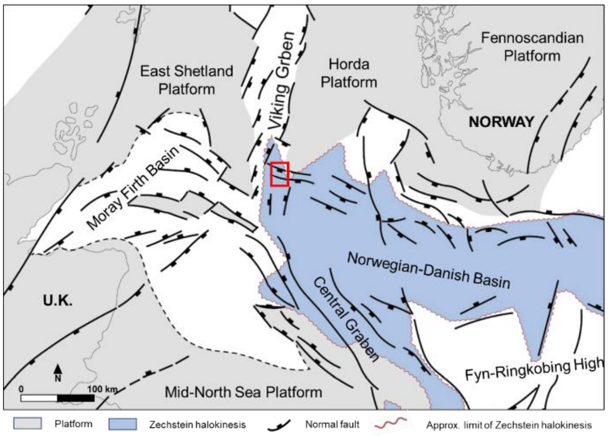

Figure 2.1. Structure elements map of North Sea. Volve field (Red rectangular) is located at the junction of Viking graben, Utsira high and Norwegian-Danish basin (modified from Pegrum, 1984).

2.2 Tectono-Stratigraphic Event

Geological stratigraphy of Volve field is the same as in Norwegian sector of South Viking Graben in the North Sea. The key sections in this study are from Upper Permian to Upper Jurassic sections. The tectono-stratigraphic events in South Viking Graben are summarized as the follows:

The South Viking Graben was formed during periods of crustal extension. The Graben Boundary Fault Zone was formed in the west of main basin structure. The beginning of extension and fault-controlled basin subsidence occurred in the Early-Late Permian (Gabrielsen et al. 1990; Coward 1995).

The Rotilegendes Group is a Lower Permian age unit. Lithology of this group is interbedded red sandstones and breccia which is related to fluvial-lacustrine to terrestrial environment. Moreover, dolomite-cement sandstone interbedded with red silty shale in some area represents more basinward facies deposition (Pegrum, 1984).

The Zechstein Group deposited during Upper Permian forms a thick succession of evaporites characterized as anhydrite and halite-rich unit and carbonate-rich unit (Pegrum & Ljones 1984; Thomas & Coward 1996). Zechstein Group distribution limited to the north-east of this area. It might have been eroded or it could be true stratigraphic pinchout.

The Zechstein salt movement started during the Triassic (Pegrum & Ljones 1984; Thomas & Coward 1996). Facies distributions during the initial phase of salt movement are non-marine Smith Bank shale dominated formation, and Skagerrak sand dominated formation (Pegrum & Ljones 1984; Fisher & Mudge 1990). The salt mobility result in varying the thickness in the unit and causes the development of a series of low-relief pillow-like features.

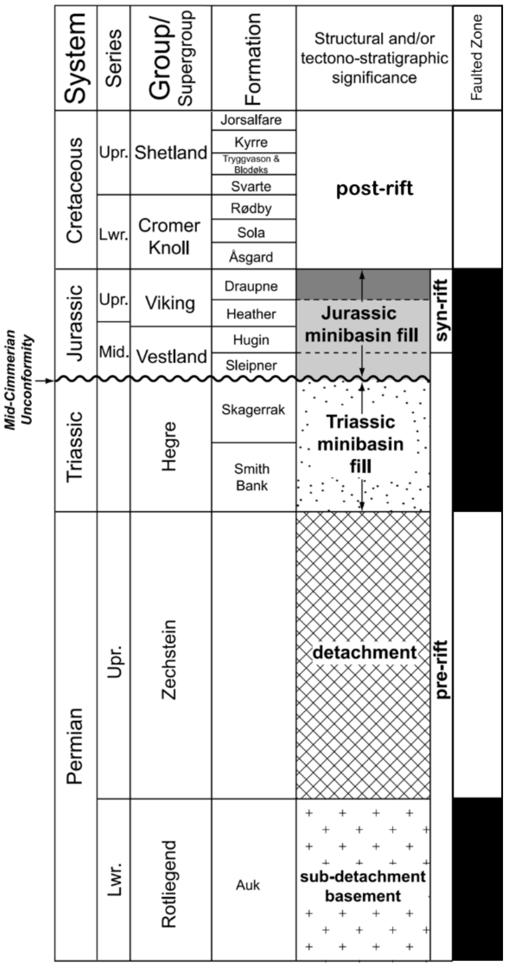

Figure 2.2. Composite stratigraphic column for the Norwegian sector of the northern part of the South Viking Graben (modified from Jackson, 2010).

During the Early Jurassic, the formation of the Mid-North Sea Dome caused the uplift and the erosion of the South Viking Graben (Ziegler 1990). As a result, Early Jurassic succession is absent in the study area and the Middle Jurassic succession is separated by mid-Cimmerian unconformity. The first deposited facies on the unconformity are delta plain deposits of Sleipner formation during Late Bajocian to Late Bathonian.

During the Middle Jurassic, the Graben Boundary fault zone was active caused by collapsing of the Mid-North Sea Dome. Consequently, the rapid subsidence and an associated marine transgression occurred in the South Viking Graben (Ziegler 1990; Thomas & Coward 1996). The initial phase of rifting in this area was the shallow marine environment. The Hugin formation (Early Callovian–Middle Callovian) was deposited during the period on Sleipner formation.

During Oxfordian to Volgian was the main phase of extension and subsidence Consequently, the eustatic sea level raised and shelf mudstones of the Heather formation and deep marine mudstones of the Draupne formation deposited.

The latest phase of extension and subsidence happened during the Late Volgian to Ryazanian, there are the inversion structures in some part of the basin (Thomas & Coward 1996; Jackson & Larsen 2008).

The post-rift deposition started during an inversion period in Early Cretaceous after the end of rifting and salt movement. The deposited sediments during this period were marine shale, marl and siltstone. The Upper Cretaceous sediment was dominantly chalk (Pegrum, 1984). During Cenozoic to Quaternary, the depositional environments relates to marine deposition.

2.3 Triassic and Jurassic Minibasin Developments

Triassic minibasin development

The study area is located in the southwest of Utsira high which is associated with the complex morphology of salt related highs and adjacent basins. A rate of deposition of Early Triassic Smith Bank Formation lacustrine mudstones may cause variable loading and the salt movement within Zechstein Supergroup (Figure 2.3a, 2.3b).

Salt mobilization of the Zechstein supergroup cause salt body growth and minibasin deepening into the depleted salt during deposition of Late Triassic Skagerrak Formation (Hodgson et al, 1992). Normally, the high sedimentation rate associated with non-marine settings and the accommodations are relatively rapidly filled. Therefore, the significant topography formed during the Triassic.

The Triassic minibasin was interrupted by the development of the North Sea Dome and the Mid-Cimmerian Unconformity during the Early Jurassic. The impact of this event led to variable erosion of the Triassic minibasins and adjacent salt bodies.

Jurassic minibasin development

Seismic data shows clearly that salt-driven subsidence patterns are different during the Jurassic compared to the Triassic minibasin development. The important features show that the salt core structure highs were places of low accommodation capped by a relatively thin Triassic succession, that then became an area of minibasin formation and accommodation during the Jurassic (Figure 5.1).

The salt body collapsed or withdrawal during the Jurassic is considered responding to the internal deformation of earlier-formed Triassic minibasin. The margins of salt formation were rotated downward, thus the original onlaps turned into downlap in present time. However, these downlap can be primary depositional feature related to the cliniform development within the Triassic succession. The clinoforms are larger than 100 m high and are probably not developed during the deposition of the predominantly lacustrine and fluvial units which would form as a flat lying event with limited accommodation space. The clinoforms are developed in areas with changing accommodation space where the space is infilled which was identified as the Smith Bank and Skagerrak Formations.

Based on the mechano-stratigraphy, there are three salt-influence mechanisms which are proposed for the Jurassic minibasin generation in the southwest of Utsira High area; salt dissolution, early Middle Jurassic erosion and salt remigration.

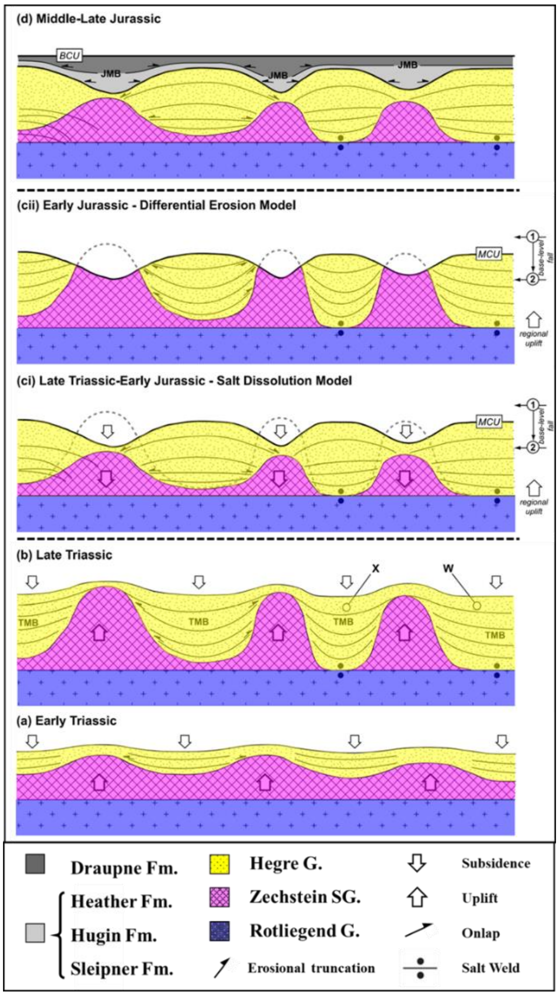

Figure 2.3. The schematic of Triassic and Jurassic minibasin associated with salt movement on the SW margin of the UH (modified from Jackson, 2010).

3. Data Availability

This study focuses on identifying the fault system related to salt movement by using seismic attributes. Seismic data was acquired in 2010 by using Ocean Bottom Cable surveys and processed in 2011 (Figure 3.1). The seismic data consist of full stack, near stack, mid stack and far stack of pre-stack depth migration. The study area covers approximately about 11 km2 which is one-fourth of seismic data area. Time interval of seismic data is down to 3400 millisecond two-way time (ms TWT).

The seismic data is normal polarity, zero phase and composes of line spacing 12.5 m in both inline and crossline direction. The frequency of seismic data ranges from 5-70 Hz (2- 3.4 seconds) with the dominant frequency of full stack, near stack, mid stack and far stack data; 25Hz, 25Hz, 25Hz and 10 Hz. respectively (Fig 3.2).

The reflectors of near stack data show similar structure as full stack data. Moreover, they have higher amplitude and more continuous reflections than the reflectors in far stack data. However, main seismic volume used in this study is full stack data due to the presence of low and high frequency in the seismic data.

Well data in Volve field focus on Jurassic and Triassic section. Therefore, the deepest wells were penetrated on Smith Bank formation over age Zechstien Salt layer. The well data 15/9-19A, 15/9-F1A, 15/9-F1B and 15/9-F4 were used for well tie to seismic.

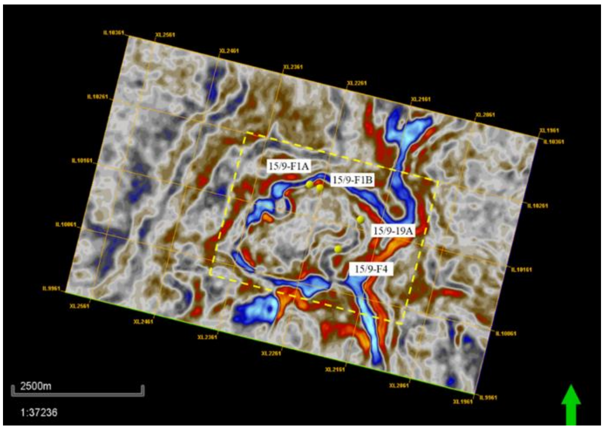

Figure 3.1. 3D seismic data of Volve filed and wells. The study area is in the yellow polygon.

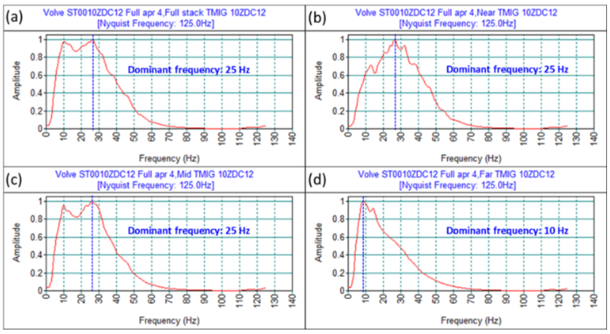

Figure 3.2. Frequency spectrum of full stack(a), near stack(b), mid stack(c) and far stack data(d) from 2 to 3.4 second interval.

4. Methodology

This study focuses on Volve anticline structure in Triassic and Jurassic section caused by Zechstien salt movement. Volve field data were reviewed by both seismic data and well data in order to interpret main horizons and fault system by using seismic attributes. The study is performed by the application of Petrel Software 2017. For horizons interpretation, there are seven key surfaces interpreted. The interpretation of faults is challenging so seismic attributes are used to help supporting the interpretation.

This study applies seismic attributes in order to improve the visuality of stratigraphic layers and fault images. The workflow is shown in Figure 4.1. Moreover, the Petrel manual was used as the reference in this part.

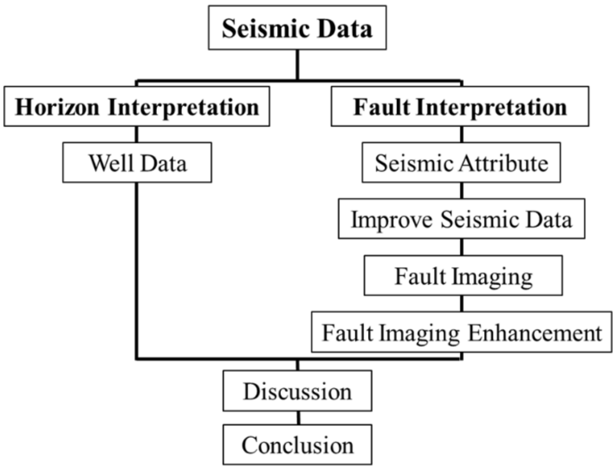

Figure 4.1. Imaging fracture and fault workflow.

5. Horizon Interpretation

In the study area, there are seven key stratigraphic surfaces identified during Late Permian to Cretaceous (Figure 5.1). The surfaces define major change in lithology and seismic characters such as seismic velocity and density.

Top Shetland formation is easily mapped in this field due to the strong reflector and good continuity. This surface represents top Cretaceous and was picked as a strong peak reflector (Red) which has high positive reflective coefficient due to the enhancement of acoustic impedance caused by the difference density of lithology between Tertiary sandstone and shale to Cretaceous chalk.

The Base Cretaceous Unconformity (BCU) is on the Jurassic Draupne formation. This surface is also easy to map owing to a strong reflector and good continuity. The strong blue trough represents a negative reflective coefficient because of decreasing acoustic impedance on the top of Draupne formation which change in lithology density from Cretaceous limestone to Upper Jurassic shale.

Top Hugin formation is difficult to map due to tectonic and salt activity during Middle Jurassic. The reflector representing this surface is a trough on the seismic data. The lithology changes from claystone with carbonate layer in Heather and Draupne formation to sandstone in Hugin formation

Top Sleipner and top Hugin reflectors are defined by well markers in the eastern flank of Volve structure. Top Sleipner horizon is picked on a peak reflector in seismic data and on coal layer in well data correlation.

The Mid-Cimmerian Unconformity is a surface between Sleipner formation and Skagerrak formation. Skagerrak formation deposited in a coalescing and prograding system of alluvial fans (NPD,2019) along the flanks while depositional environment of Sleipner formation is fluvial deltaic. The MCU reflector is weak and discontinuous reflector due to erosion and uplift activity. It is picked on a trough reflector that is tied to well data.

For the top of salt section, there is no well penetrated into Zechstein group. However, Sleipner East field has well (15/9-9) penetrating into Zechstein group and top of Rotliegend formation. The lithology of Zechstein group consists of dolomite, gypsum, anhydrite, and occasionally shale and marl. The Rotliegend formation contains sandstone and some breccia. The acoustic impedance increases due to the contrast between Smith Bank shale and Zechstein salt causing a high positive reflective coefficient. Therefore, Top Zechstein group is picked on the strong red peak reflector. The top Rotliegend formation, is picked on the trough reflector at the interface between Rotliegend sandstone and Zechstein salt.

6. Fault Interpretation

Volve anticline structure was formed by Zechstien salt movement during Triassic and Jurassic period and the fracture and fault were created in Triassic and Jurassic section. The seismic data in Triassic and Jurassic sections present as blurred (Fig 6.1) and chaotic reflectors and it could not detect fracture and fault in this section due to discontinuous reflectors. Therefore, seismic attributes were applied to help identifying fractures and faults in Volve anticline.

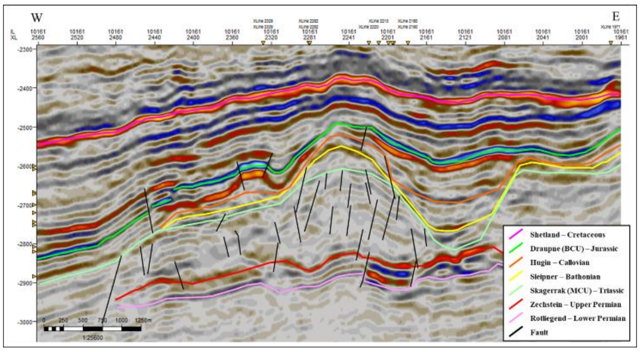

Figure 5.1. The seven-key surfaces of the Volve field in W-E section line.

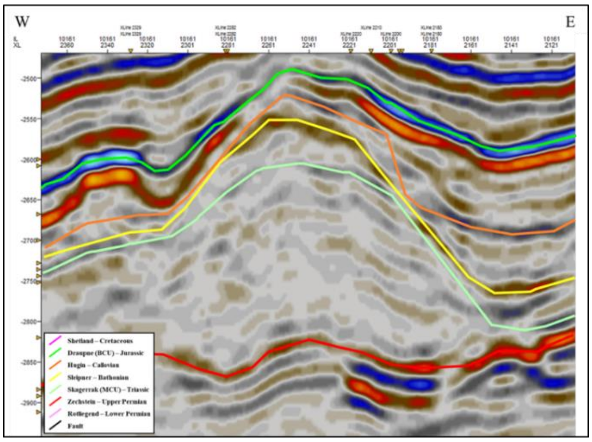

Figure 6.1. The blurred and uncleared reflectors in Triassic and Jurassic section on cross-section IL 10161.

6.1 Improved Seismic Data

The first step is to improve the seismic data and reduce random noise by using median filter. This attribute has three parameters which are the filtering window size in three dimensions. It is to run through the signal entry by entry and replacing each entry with the median of neighboring entries. This technique helps smoothing values in between seismic data and preserving reflector edge information of seismic data. The result of median filter attribute is almost the same as the original. It is slightly clearer reflector in the blur zone.

6.2 Fault Imaging

After improving seismic data, Fault imaging attributes were tested. Variance and Chaos attributes are mostly used to produce fault imaging.

The variance attribute evaluates the discontinuities in the horizontal continuity of amplitude. It estimates local variance in the signal. This method isolates edge effects in the seismic data set. The variance with dip-guidance is useful for highlighting structural features such as faults because it will be easy to detect discontinuity of fault feature along the dipping of the reflector. In contrast, the variance without dip guidance is useful for accentuating stratigraphic feature such as channels. Channel feature on the seismic normally cut through other reflector as a cup-like feature, thus without dip guidance it will be easier to detect discontinuity of stratigraphic feature.

For the chaos attribute, this method evaluates chaotic signal pattern that is lack of organization in the dip and azimuth estimation method. The chaos in the signal can be used to illuminate faults and geological feature such as gas migration path, salt body, and channel infill. The results of both attributes show groups of small subtle faults altogether at the Volve anticline area (Figure 6.2). The fault images of both attributes may be caused from the discontinuity of stratigraphic succession moved during salt movement or they may have a lot of fault and fracture in the zone.

Variance attribute produced clearer fault images than Chaos attribute. The reason for this is Chaos attribute produce blurred images and resulted in a decrease in fault images. Therefore, edge enhancement was applied to improve fault image of Variance volume.

6.3 Fault Image Enhancement

The Variance volume is not good at fault imaging because it has noise and influenced by stratigraphic features. Edge Evidence and Ant-tracking attributes were applied to Variance volume in order to sharpen and add details to fault images.

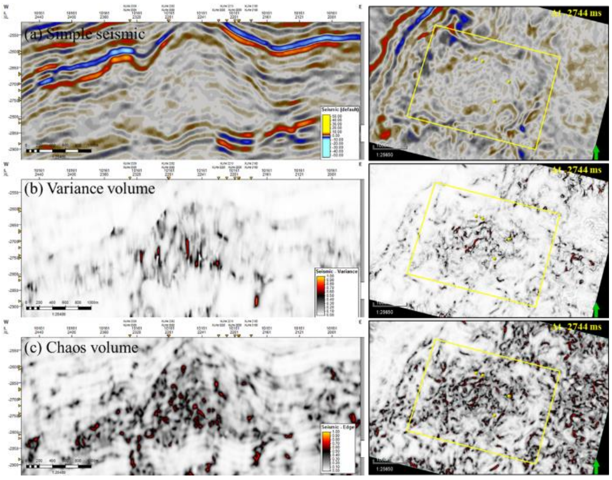

Figure 6.2. The cross-section and time slice of simple seismic (a), Variance (b) and Chaos attributes (c). The fault image of Variance attribute presenting the trend of fault feature compared to Chaos attribute presenting blur spots of discontinuity

Edge Evidence attribute was applied to enhance fault image of Variance volume. A statistic edge enhancement method is used to define fault and salt body border within seismic data. The Edge Evidence works by searching locally in all directions for line segments where the values on the line differ significantly from the surrounding values. The result is the best evidence of a line passing through that point.

The result of Edge Evidence volume shows clearer fault images than the Variance volume (Figure 6.3a). The fault image shows very thick fault layers which may represent combined smaller faults that are below seismic resolution causing unclear fault image on the time slice; on the contrary, fault image is clearer in the cross-section. In this process, the stratigraphic feature was removed by using a filter that removes horizontal stratigraphic reflections resulting in an emphasis on imaging of the fault surface.

The next step is to sharpen fault image extraction and fine tune the detail of fault surface image using Ant-Tracking attribute. The ant-tracking attribute is a powerful edge enhancement tool applied to others fault-sensitive attributes. The ant-tracking algorithm is a directionally controlled auto picker based on the idea of ant-colony systems to capturing trends in noisy data. This approach enhances the discontinuities in an edge-detection volume because it only captures features that are continuous and likely to be faults. After the data has been conditioned by removing horizontal reflections. Normally, the ant tracking algorithm does not capture non-structural features such as noise and channels due to these features generally have internally chaotic textures and do not form continuous high angle linear features which are the faults, which are not continuous, and prevent the ant-tracker from extracting these non-surface-shaped features. The result of this attribute shows fault zones sharply and greatly in details.

The result of Ant-Tracking volume shows very clear and detailed faults (Figure6.3b). There are many fault orientations caused by salt movement. In the study interval, fault surface mostly presented in the Triassic section because the most salt movement activity occurred at that time. In addition, the fault surface occasionally presented in the Zechstein and Jurassic sections, and rarely presented in the Cretaceous section.

As a result, the workflow process and resulting attributes applied to seismic data enhanced the fault image in Volve field. It indicates the main faults occur in western part of the field. Moreover, fault orientations caused by Zechstein salt movement are in NE-SW and NW-SE direction. Most faults are present in the Jurassic section and Permian clastic sections.

6.4 Automatic Fault Extraction

Automatic fault extraction method (AFE) is the technique to extract, display, analyze and edit fault-patches. The result of fault-patch extraction is a discontinuous surface. Only short-disconnected fault segments are seen after fault patches extraction from Ant-Tracking attribute. Therefore, they need to be merged in a geological sense along the entire expected fault plane.

AFE extract fault patches from Ant-Tracking attribute volume by creating fault patches along trends of the highest value. A quantity of fault-patches extraction depends on the confidence threshold. When a low value of the confidence threshold is set, the extracted noise and fracture will increase. In reverse, too high a confidence threshold can cause missing fault-patches from extraction.

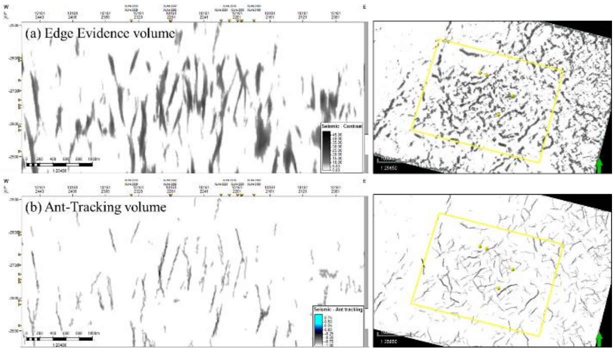

Figure 6.3. The fault images of Edge Evidence (a) and Ant-Tracking (b) attributes. The Ant-Tracking volume shows fault image sharply and greatly in details.

The results of AFE show that it does not work for this field because there are many fault patches with many orientations and geologically they may not be continuous. Moreover, the fault value in the Ant-Tracking volume is low causing the extraction of non-logic fault patches (Figure 6.4).

Figure 6.4a illustrates the result of AFE with high confidence threshold and Figure 6.4b illustrates the result of AFE with normal confidence threshold. Both cannot extract fault-patches properly.

For instance, a fault patch with the normal confidence threshold (Figure 6.5) shows better geological concept and present fault patch along with the fault image in Ant-Tracking attribute while it compares to a fault patch with the high confidence threshold. The fault patch with the high confidence threshold presents only a fault segment that does not represent geological concept. However, both of them do not extract the fault patches properly.

Therefore, Fault-patches were extracted by manual fault interpretation in the focus area using geological concepts instead of computer forced interpretation (Figure 6.4c).

7. Discussion

From the studied results, the faults image in the Ant-Tracking volume shows that fault dominates in Triassic section. The main fault orientation is northeast to southwest and the orientation are northwest to southeast and north-northeast to south-southwest. The main fault orientation of this field has major fault trend the same as in South Viking Graben. The activity of Zechstein salt movement caused many faults in the Volve field.

The understanding of fault orientation in the Volve field is presented by the Ant-Tracking time slice with fault azimuth rose diagram and by cross-section (Figure7.2).

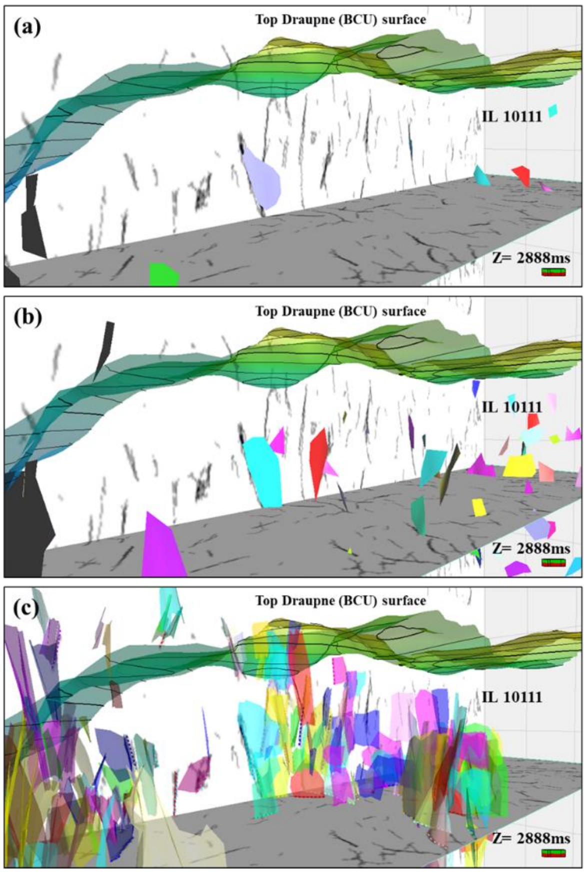

Figure 6.4. The result of automatic fault extraction (AFE) in 3D. (a) The result of AFE with high confidence, (b) The result of AFE with low confidence, and (c) The manual fault interpretation from Ant-Tracking volume.

In the late Permian, a thick salt package (Zechstein group) was deposited across the area. It was overlaid by Triassic sediment (Smith Bank and Skagerrak formation). The salt started mobilizing, forming depocenter in the area of withdrawal, and creating salt ridges and diapirs in nearby areas. The salt movement led to significant differences in subsidence. Faulting and salt movement were further accelerated by extensional tectonics which is related to the opening of the Viking Graben (Figure 7.1a). In the seismic section, many of the faults and fractures present in the Triassic section are caused by salt activity during Triassic and Jurassic periods.

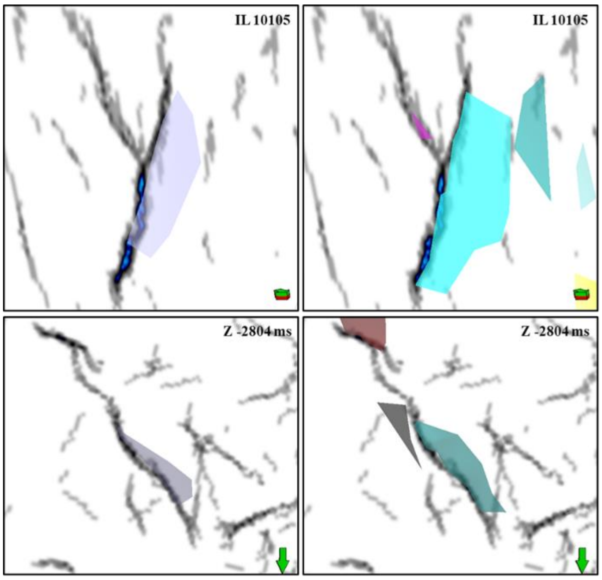

(a) High confidence threshold (b) Normal confidence threshold

Figure 6.5. Comparison of automatic fault extraction result between (a) high confidence threshold and (b) normal confidence threshold.

In the Upper Permian section (below Zechstein salt section), the fault images are clearly seen on the Ant-Tracking attribute (Figure 7.3e and 7.3f). The fault azimuth direction in this section presents in the northeast to southwest and northwest to southeast directions. However, in the northeast to southwest section, the fault azimuth direction of Permian section presents more angle than Triassic-Jurassic section. Mostly the fault azimuth is around 60 degree with narrow azimuth range (50 to 70 degree).

In the Triassic sections, the Ant-Tracking attribute shows clearly fault image because Volve anticline structure is surrounded by Cretaceous section (white space) (Figure 7.3b, 7.3c and 7.3d). The Ant-Tracking attribute shows fault azimuth mostly in the direction of northeast to southwest and northwest to southeast. The major azimuth direction is around 45 degree and the range is approximately 30 to 60 degree. The minor fault azimuth is around 330 degree and the range is approximately 315 to 345 degree.

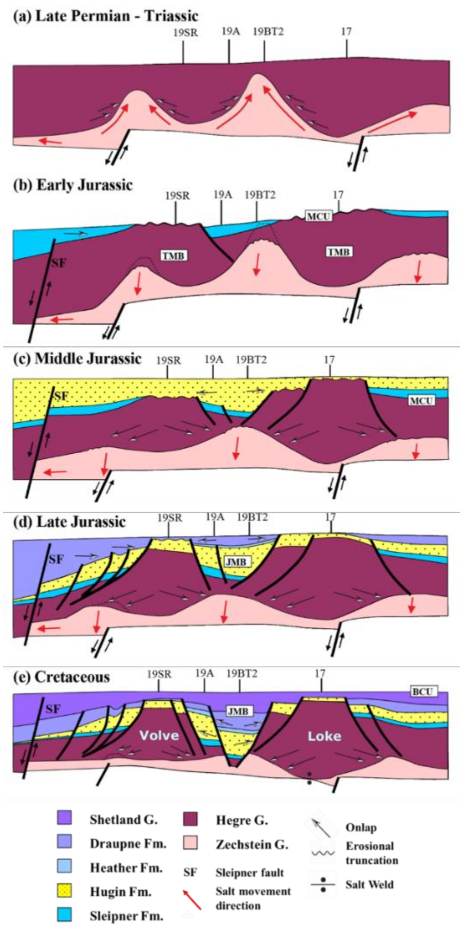

Figure 7.1. Schematic illustration of the Volve field

Jurassic deposition initially occurred in a coastal plain situated on extensive coal mires and swamp areas (Sleipner Formation). The shallow marine of Hugin formation deposited in the Middle Jurassic (Callovian time) (Figure 7.1c). It filled thick sand in subsiding area while thinner sand layers were deposited on the highs. After that, the sea level rose, it caused a marine deposition Heather formation. More constrained marine conditions resulted in high organic productivity in deposition of the Draupne formation. The Ant-Tracking attribute in the Jurassic section show a small number of faults (Figure 7.3). It indicates that there is low tectonic activity during the forming of the Jurassic minibasin which is supported by the previous interpretation about the mechanism of Jurassic minibasin generation.

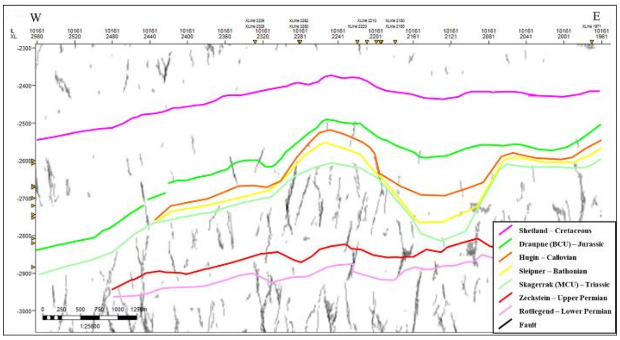

Figure 7.2. The cross-section of the Ant-Tracking attribute on IL 10161 which has top of stratigraphic surface.

During Late Jurassic to Early Cretaceous (Figure 7.1d and 7.1e)., the occurrence of salt dissolution caused thick packages of marine shale units depositing above the former salt diapirs. The Triassic highs have very few shales in Upper Jurassic formation. Continuous subsidence in Cretaceous and Tertiary times resulted in thick packages of shale, sandstone and chalk deposited above the Volve structure. There are minor faults present in Ant-Tracking time slice (Fig 7.3a) because there is a lack of major reflection in lithology to show offsetting reflectors that are evidence of fault. The Lower Cretaceous deposited in deep marine environment which has lithology as marine shale and calcareous claystone layers. For the Upper Cretaceous, it deposited in open marine and it consists of limestone, chalky limestone and lime-mudstone.

The difference between the azimuth of Triassic-Jurassic and Upper Permian sections may be caused by salt body pop up during Triassic-Jurassic period or there was change in regional stress directions at this time.

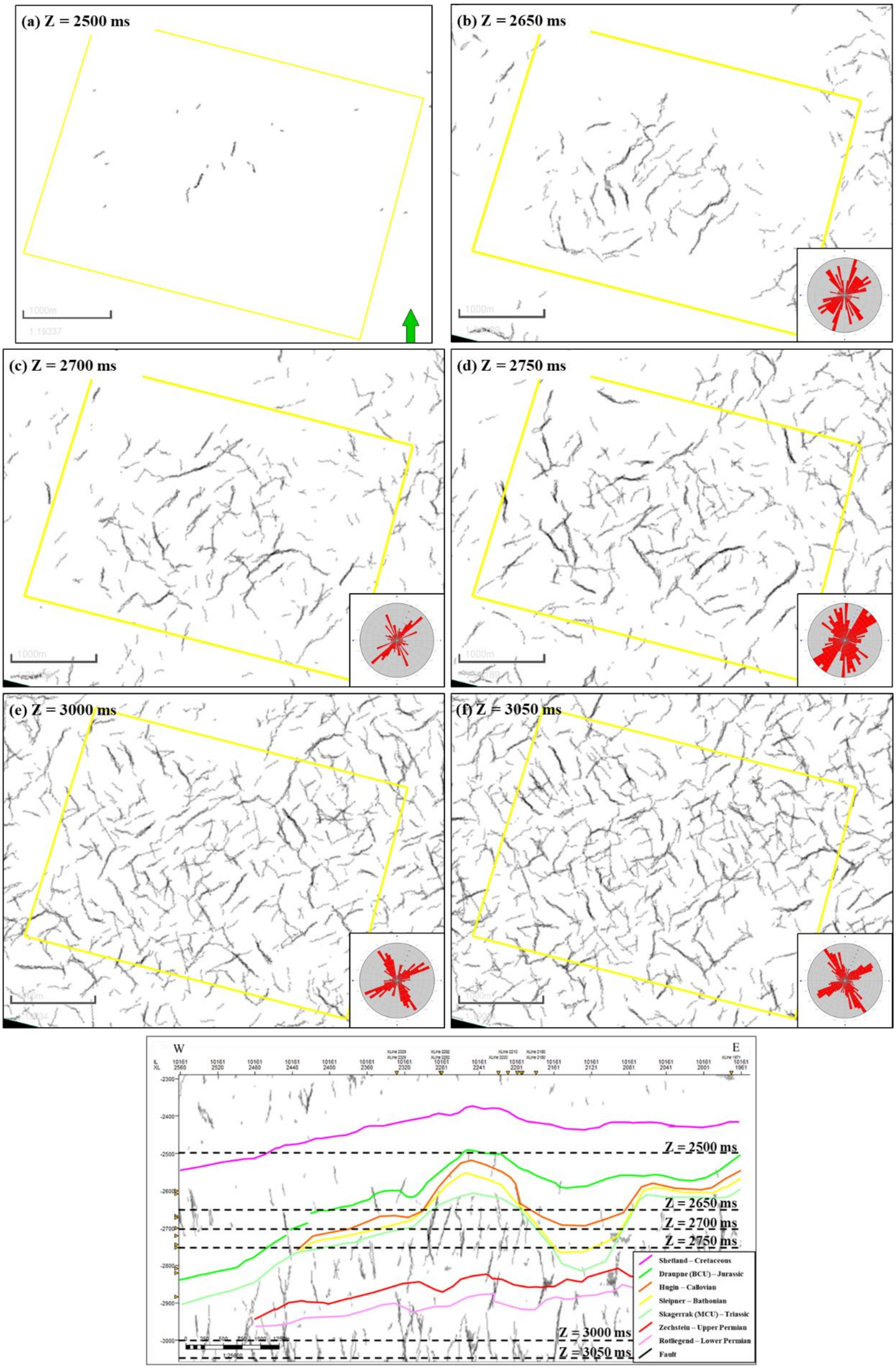

Figure 7.3. The Ant-Tracking attribute time slice at 2.50,2.65, 2.70, 2.75, 3.00 and 3.05 second and cross-section of IL 10161.

8. Conclusion

The analysis of the 3D seismic data provided a detailed understanding of the fault system in the field. Key conclusions from study are the following:

1) Seismic attribute assisted the seismic data to reveals the fault image of the Volve, it needs to follow the workflow from fault imaging to enhance fault imaging and extract fault-patch.

2) Automatic Fault Extraction does not work for this field because the fault value in the Ant-Tracking attribute is very low. Therefore, the fault-patches that were extracted do not relate to the geology.

3) The main fault development is in the Triassic section because the minibasin configuration changed during salt growth in Triassic period. There is a lack of fault development in the Jurassic section because of low tectonic or salt activity during the Jurassic formation deposition. For the Cretaceous section, it has no fault in the Volve field area because there is a lack of major reflection in lithology to show offsetting reflectors that are evidence of fault.

4) Seismic attribute reveals the presence of the two dominate orientation of faulting: Northeast to southwest and northwest to southeast. Fault orientations in the Triassic section and Early Permian sections are different from the fault trends of the Late Permian section.

5) This methodology can be used for fractured basement evaluation in further study or application to other field that have difficult to see faults or fractures.

10. Acknowledgement

The author would like to express my gratitude to all those who give the opportunity to study in Petroleum geoscience program and perform this research in Chulalongkorn University. Thank to PTT Exploration and Production Ltd. for fully support in M.Sc. scholarship. Thanks to Professor Angus John Ferguson for supervision, suggestion, recommendations and support during this research project.

11. Reference

Coward, M.P. 1995. Structural and tectonic setting of the Permo-Triassic basins of northwest Europe. In: Boldy, S.A.R. (ed.) Permian and Triassic Rifting in Northwest Europe. Geological Society, London, Special Publication, 91, 7–39.

Fisher, M.J. & Mudge, D.C. 1990. Triassic. In: Glennie, K.W. (ed.) Introduction to the Petroleum Geology of the North Sea. Blackwell, Oxford, 191–218.

Gabrielsen, R.H., Færseth, R.B., Steel, R.J., Idil, S. & Kløvjan, O.S. 1990. Architectural styles of basin fill in the northern Viking Graben. In: Blundell, D.J. & Gibbs, A.D. (eds) Tectonic Evolution of the North Sea Rifts. International Lithosphere Programme, 81, 158–179.

Hudec, M.R. & Jackson, M.P.A. 2007. Terra infirma: Understanding salt tectonics. Earth-Science Reviews, 82, 1–28.

Jackson, C. A. L., K. E. Kane, and E. Larsen, 2010, Structural evolution of minibasins on the Utsira High, northern North Sea; implications for Jurassic sediment dispersal and reservoir distribution: Petroleum Geoscience, v. 16, p. 105-120.

Pegrum, R.M. & Ljones, T.E. 1984. 15/9 Gamma gas field offshore Norway, new trap type for North Sea Basin with regional structural implications. American Association of Petroleum Geologists Bulletin, 68, 874–902.

Thomas, D.W. & Coward, M.P. 1996. Mesozoic regional tectonics and South Viking Graben formation: evidence for localized thin-skinned detachments during rift development and inversion. Marine and Petroleum Geology, 13, 149–177.

Ziegler, P.A. 1990. Tectonic and palaeogeographic development of the North Sea rift system. In: Blundell, D.J. & Gibbs, A.D. (eds) Tectonic Evolution of the North Sea Rifts. International Lithosphere Programme, 81, 1–36.